The Influences of Fiber Feature and Polymer Melt Index on Mechanical Properties of Sugarcane Fiber/Polymer Composites

John Z. Lu,[1] Qinglin Wu,[2] Ioan I. Negulescu,[3] Yan Chen[3]

[1]*Department of Wood Science and Engineering, Oregon State University, Corvallis, Oregon 97331*
[2]*School of Renewable Natural Resources, Louisiana State University Agricultural Center, Baton Rouge, Louisiana 70803*
[3]*School of Human Ecology, Louisiana State University Agricultural Center, Baton Rouge, Louisiana 70803*

Received 16 March 2006; accepted 16 April 2006
DOI 10.1002/app.24929
Published online in Wiley InterScience (www.interscience.wiley.com).

ABSTRACT: The fiber characteristics (i.e., the fiber type, morphology, and dimension) and polymer melt flow index (MFI) significantly affected mechanical properties of sugarcane fiber/HDPE composites. The length and diameter of sugarcane fibers followed a lognormal distribution before and after compounding. The long fibers had a significant reduction in the dimension and aspect ratio during compounding. However, the short fibers had close values in these two properties before and after compounding. For the resultant sugarcane fiber/polymer composites, the HDPE resins with a low MFI value presented high tensile and impact strengths. Because of high sugar content, the pure rind fiber had a poor performance as filler in the HDPE resins with respect to the raw bagasse fiber and alkali-extracted bagasse fiber. On the other hand, the aspect ratio was proportional to the mechanical performance of the fibers in the HDPE resins. As a result, the fibers with a large aspect ratio and low sucrose content improved the strength properties of the resultant composites. © 2006 Wiley Periodicals, Inc. J Appl Polym Sci 102: 5607–5619, 2006

Key words: sugarcane fibers; composites; fiber dimension and aspect ratio; melt flow index; HDPE

INTRODUCTION

Sugarcane is an important agricultural crop in the Southern United States. It is estimated that the US sugar industry mills over 35 million tons of green cane each year to produce sugar and related products.[1] Concurrently, the sugar industry generates over 4.5 million tons of dry fibrous materials (i.e., sugarcane bagasse) per year as its by-products.

Sugarcane stems consist of internodes, nodes, lateral buds, and leaf blades and sheaths.[2,3] On the cross section of each stem, the outer portion mainly contains cortex or rind, whereas a large mass of storage tissue (parenchyma, mainly for sucrose storage) is the primary part of the internal portion. The sucrose content in the parenchyma (or pith) is as high as 14%, but the rind part contains relatively low sucrose.[2]

Sugarcane bagasse (or bagasse) is the fibrous residual material of the sugarcane stems left after the crushing and extraction process from sugar mills, which normally accounts for 20–24% of the cane.[3,4] As the main sources of sugarcane fibers, bagasee usually consists of rind, vascular bundles, and pith (the parenchyma). It contains cellulose (46.0%), hemicellulose (24.5%), lignin (19.95%), fat and waxes (3.5%), ash (2.4%), silica (2.0%), and other elements (1.7%).[5] In the rind part, cellulose fibers account for 50%, while lignin and hemicellulose are 18 and 30%, respectively.[6] It is estimated that the output of bagasse fibers are 75 million metric tons worldwide per year.[7]

As early as in the 1950s, bagasse has been extensively used as an industrial raw material. In general, bagasse can be used for cellulose, plastics, fermentation products, cane wax, paper and pulps, insulating board, particleboard, filter mud or cake as a field fertilizer, and sucrose and sucrose-based organic products.[3,8] However, most of bagasse is burned as a fuel in sugar mills to reduce its environmental problems.

Since the 1990s, more attention has been paid to the value-added applications of sugarcane fibers in bio-based composites. In the USDA Forest Products Laboratory (FPL) at Madison, WI, much effort has been made to combine wood and nonwood plant fibers (e.g., bagasse, kenaf, jute, and hemp) with thermoplastic fibers to manufacture natural fiber/polymer composites by the nonwoven process.[9,10] Rowell and Keany[11] studied the fabrication of bagasse board using acetylated bagasse fiber. Thus far, a number of research articles on sugarcane bagasse-based composites as value-added products have been published worldwide.[12–17]

Correspondence to: J. Z. Lu (johnzlu@yahoo.com).
Contract grant sponsor: Louisiana Governor's Biotechnology Initiative Program ; contract grant number: 101-40-0120.

Collier and colleagues[18,19] investigated the potentiality and feasibility of using bagasse fiber as geotextile products. Based on their studies, a patent on a process to separate cellulose fiber from the plant stalk rind was issued in 1998.[20] Chen et al.[21,22] developed a nonwoven process to manufacture bagasse/polymer composites for the potential applications in automobile industry. More recently, Han and Wu[23] investigated the anatomical features, thermal, moisture sorption, and tensile strength properties of sugarcane rind flakes in comparison with wood flakes. The result showed that strand composites made from rind flakes had better strength properties and dimensional stability than those from wood flakes.

Compared with a nonwoven process, a melt-blending process has a low cost and high efficiency in production. A number of publications on melt-blended nonwood fiber/polymer composites have been reported.[24,25] In the current study, a melt blending process was used to manufacture sugarcane fiber/HDPE composites. The objectives of this study were to investigate the effects of polymer melt index and fiber dimension and distribution on mechanical properties of the resultant composites.

EXPERIMENTAL

Materials

Three sugarcane fibers were used in this study to compare their performance as filler in the HDPE resins. These fibers included the raw bagasse fiber (RBF), pure rind fiber (PRF), and alkali-extracted bagasse fiber (EBF). RBF was obtained from a local sugar mill in Louisiana, which had been stored outdoors for over one year.[22] PRF was produced by passing canes through a Tilby cane separator (Tilby Systems, British Columbia, Canada) to extract rind from the cane stalk. To make EBF, raw bagasse was first boiled in 1*N* NaOH solution for 4 h to remove the most of hemicellulose, lignin, and sucrose residuals. Alkali-extracted fiber was then rinsed with water for 3–4 times and dried in an oven at 70°C for 72 h.[22] The yield of EBF was about 50% on average after alkali extraction.

Four different HDPE pellets were obtained from Golden Chemical Company, Houston, TX (a merchant dealer of Exxon-Mobile Company, Houston, TX). Basic properties of these thermoplastic resins are listed in Table I. All the as received HDPE resins have a density close to 950 kg/m^3. The mechanical properties of these resins are directly related to the melt flow index (MFI) values. Among these resins, HD9856B has the highest tensile and impact strengths, while HD6733 has the lowest strengths (Table I).

Fiber grinding and screening

Before grinding, all the fibers were oven-dried at 80°C for 24 h. The moisture content of oven-dried fiber was between 3 and 5%. All the oven-dried fibers were first ground with a Thomas–Wiley miller (Model 3383L10, Swedesboro, NJ) to pass through a 10-mm screen. All the ground fibers were sorted with 20 and 60 mesh screens, respectively, and divided into three fiber fractions in dimension: (1) the fibers not passing the 20 mesh screen (defined as +20# or < 20#), (2) the fibers passing the 20 mesh screen but retained on the 60 mesh screen (defined as −20/+60# or 20/60#), and (3) the fibers passing the 60 mesh screen (defined as −60# or > 60#). All the sorted fibers were placed in sealed plastic bags before compounding.

Determination of sugar content in sugarcane fibers

A high-performance liquid chromatograph (HPLC) system was used to determine the sugar content in the fibers. This system consists of a Shodex RI71 detector (J M Science, Grand Island, NY), a PC with Dionex Peaknet 5.01 and UI20 universal interface for integration (Dionex, Sunnyvale, CA), a Bio-Rad AS 100 HPLC autosampler (Bio-Rad Laboratories, Hercules, CA), and a Waters® 515 pump (Waters, Milford, MA). The HPX-87K column (Bio-Rad Laboratories) had a dimensional size of 300 mm in length and 7.8 mm in

TABLE I
Properties of HDPE Resins as Received

Resin	Melt flow index (g/10 min)	Density (kg/m^3)	Melting temperature (°C)	Tensile strength (MPa)	Tensile impact (J/cm^2)
HD9856B	0.46	957	–	30.0	–
HD6761	6.1	952	132	24.7	349 (77.0)
HD6714	14.0	951	131	23.0	333 (60.3)
HD6733	33.0	950	129	21.8	210 (45.0)

All above data were provided by Exxon-Mobile Company. These properties are determined according to the following ASTM standards: ASTM D 1238 for melt flow index, ASTM D 4883 for density, ASTM D 3418 for melting point, ASTM D 638 for tensile strength, and ASTM D 1822 for tensile impact.

diameter. During testing, the column was heated at 85°C and the moving phase of 0.01*M* K_2SO_4 run at 0.6 mL/min.

For analysis of sugar content, 5 g fiber samples were placed in an Erlenmeyer flask and mixed well with 50 mL distilled water. The solution was stored for 30 min and then diluted to 100 mL. Approximately one gram of the diluted sample was placed in a 100 mL volumetric flask. The sample was diluted with Type I water (i.e., purified water that has more than 18.0 MΩ cm specific resistance according to ASTM standard ASTM D1193) and filtered through a 0.45 μm filter into a sample vial. The vial was placed in the refrigerated autosampler. The solids weight, calculated from the Brix reading (i.e., a hydrometer scale for measuring the concentration of sugar solutions) of the 1 : 1 solution, was inserted into the integrator.

Before determining the sugar content in each sample, a series of calibration were conducted with three standard solutions.[26] In this study, these standards used had different composition ratios of sucrose, glucose, and fructose. The ratio of these analytes in Standard 1 was 9.977/0.918/0.912; that in Standard 2, 19.893/2.992/2.991; while that in Standard 3, 29.985/6.000/5.986. After running these standard solutions with HPLC, a linear regression for sucrose, glucose, and fructose was conducted with the external fit, respectively. The regression presented the corresponding relationship of the area under each compound retention peak with its amount in the standards. Based on the linear regression, these three compounds in the standards were quantitatively determined. In this study, all these calibration lines had a R^2 value larger than 0.9999. According to the

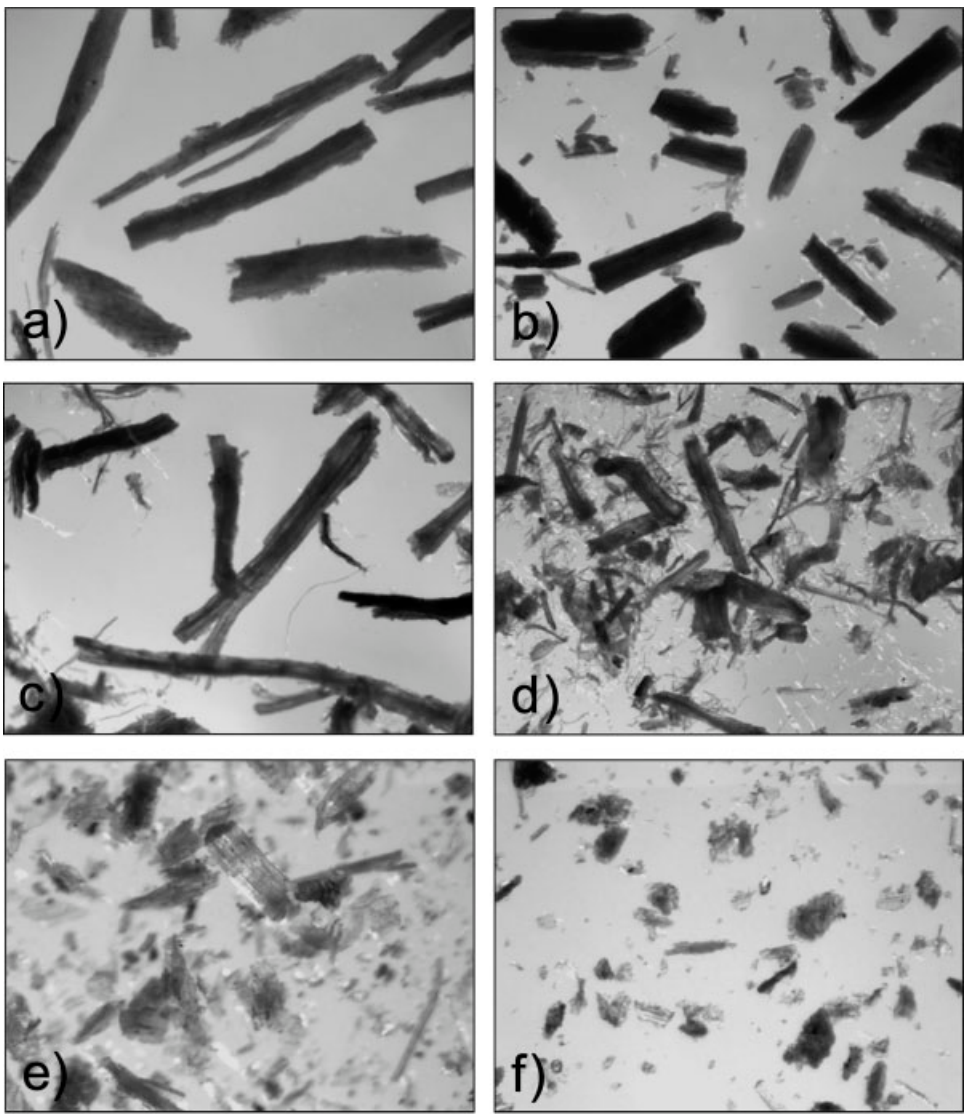

Figure 1 Imaging photographs of the sugarcane fibers. (a) +20# RBF before compounding (20×), (b) +20# RBF after compounding (20×), (c) +20# EBF before compounding (20×), (d) +20# EBF after compounding (20×), (e) −60# RBF before compounding (63×), and (f) −60# RBF after compounding (63×).

area under the peak of each compound, the composition of a sample was determined by inserting the data in the aforementioned regression for each compound.

Compounding process

The sugarcane fibers and HDPE resins were mixed in a Haake Rheomix 600 rotor mixer (Thermo Electron, Dreieich, Germany). The weight percentage of the oven-dried sugarcane fiber to HDPE was 30 wt % for all the resultant composites. The compounding process was conducted at a temperature of 165°C and a mixing time of 10 min with a rotation speed of 90 rpm.[27] After compounding, the melts were removed from the blender and cooled to room temperature.

Soxhlet extraction of sugarcane fiber–HDPE blends

After compounding, about 350 mg sugarcane fiber/HDPE blends were randomly selected and stored in the thimbles of a Soxhlet apparatus. The blends were extracted with hot xylene solution for 48 h.[28] The remaining sugarcane fibers were removed from the thimble and oven-dried at 80°C for 24 h prior to the fiber dimension measurement.

Fiber dimension measurement

An imaging system was used for the fiber dimension measurement. The system consists of a Leica MZFIII microscope (Leica Microsystems, Wetzlar, Germany), a CCD digital camera (Diagnostic Instruments, Sterling Heights, MI), a υ-Lux 1000 optical lighter (Volpi MFG USH Co., Auburn, NY), a RT SP402-115 power supply (Diagnostic Instruments), and a computer.

For the dimension measurement, 30 mg fibers before compounding were randomly selected, whereas 10 mg fibers extracted from the fiber–HDPE blends were used. All the fiber samples were evenly placed on a glass dish under the microscope and clearly focused by adjusting the height of the microscope. The optical lighter was adjusted to achieve better picture quality. With the Spot Advanced imaging software (Diagnostic Instruments), the image was recorded with the CCD digital camera and saved as a data file. The length and diameter of individual fibers were measured with the Image-ProPlus 6.0 software (Media Cybernetics, Silver Spring, MD). An aspect ratio, which is equal to the ratio of the fiber length and diameter for individual fibers, was used to evaluate the fiber reinforcement in the resultant composites.

Manufacture of sugarcane fiber–HDPE composites

The fiber–HDPE blends with a target weight were placed in a three-piece stainless molding set. The mold was pressed with a Wabash V200 hot press (Wabash, ID) at 175°C for 4 min and then cooled to room temperature under a pressure. The pressure for heating and cooling was controlled at 30 tons. For tensile testing and dynamic mechanical analysis (DMA), the nominal thickness of tensile specimens was 1 mm, while the nominal thickness for the impact strength testing specimens was 4.5 mm.

Mechanical property measurement of the resultant composites

The density profile of each composite sample was analyzed with a QMS QDP-01X density profiler (Quinteck Measurement Systems, Oak Ridge, TN). The sample dimension was 60 mm by 50 mm by thickness. The density distribution across the thickness was analyzed and plotted.

The storage modulus E' of the resultant composites was analyzed with a TA Q800 DMA system (New castle, DW). Before testing, all the DMA specimens were

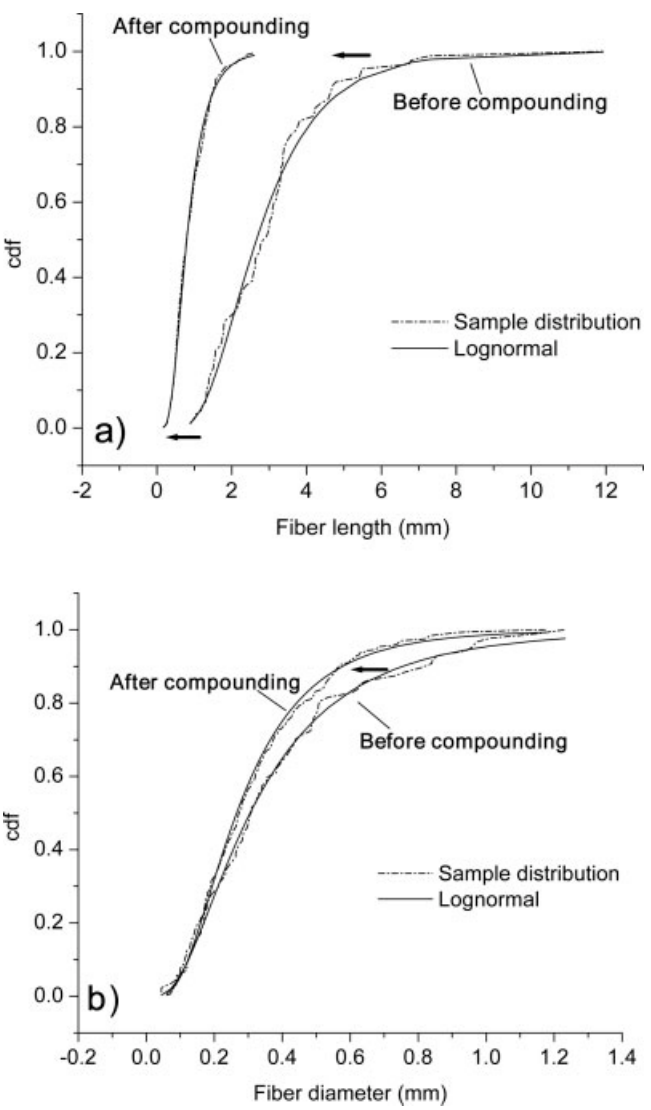

Figure 2 RBF dimension distributions before and after compounding on (a) fiber length and (b) fiber diameter.

TABLE II
Comparison of the Fiber Dimension Before and After Compounding

Sugarcane fiber	Mesh size	Sampling number	Average length (mm)	Average diameter (mm)	Average aspect ratio
Before compounding					
RBF	+20#	87	3.01	0.38	13.64
	−20/+60#	113	1.07	0.34	4.12
	−60#	118	0.38	0.16	2.66
PRF	+20#	92	2.83	0.57	6.61
	−20/+60#	111	1.15	0.34	3.89
	−60#	152	0.34	0.12	3.17
EBF	+20#	98	2.44	0.39	8.37
	−20/+60#	114	1.06	0.26	5.07
	−60#	131	0.47	0.15	3.42
After compounding[a]					
RBF	+20#	371	0.91	0.32	3.38
	−20/+60#	659	0.73	0.26	3.18
	−60#	418	0.28	0.12	2.96
PRF	+20#	432	0.81	0.24	4.00
	−20/+60#	523	0.80	0.24	3.81
	−60#	849	0.37	0.14	3.09
EBF	+20#	222	0.97	0.22	5.88
	−20/+60#	665	0.68	0.20	4.00
	−60#	582	0.38	0.12	3.15

RBF, raw bagasse fiber; PRF, pure rind fiber; and EBF, alkali-extracted bagasse fiber.
[a] The polymer matrix used was HD6714.

conditioned for 72 h at a temperature of 23°C and a relative humidity of 50%. The storage modulus of each DMA specimen was measured with a dual cantilever mode at a frequency of 1 Hz under room temperature.

After the DMA test, all the specimens were measured for tensile strength according to the ASTM standard ASTM D638. The tensile strength of each specimen was tested with an INSTRON 1125 machine (Instron, Norwood, MA). For each treatment level, six replications were conducted.

A TINIUS 92T impact tester (Testing Machine Company, Horsham, PA) was used for the Izod impact test. All the samples were notched on the center of one longitudinal side. For each sample, the nominal width was 12.7 mm and the nominal notch depth, 2.5 mm according to the ASTM Standard ASTM D256. For each treatment level, five replications were conducted.

Data analysis

A 4 × 3 × 3 completely randomized design (CRD) with a factorial arrangement was conducted to investigate the influences of MFI (0.46, 6.1, 14, and 33) and the fiber type (RBF, PRF, and EBF) and mesh size (+20#, −20/+60#, and −60#) on the mechanical properties of the resultant composites. Based on the CRD factorial experiment, a three-way analysis of variance (ANOVA) was conducted to determine the main and interaction effects on the tensile and impact strengths of the resultant composites, respectively.

RESULTS AND DISCUSSION

Fiber morphology and dimension distribution

With a small mesh size (e.g., +20#), all the sugarcane fibers had a cylindrical tube or granule shape before and after compounding [Figs. 1(a) and 1(b)]. Compared with RBF and PRF, EBF was flexible and usu-

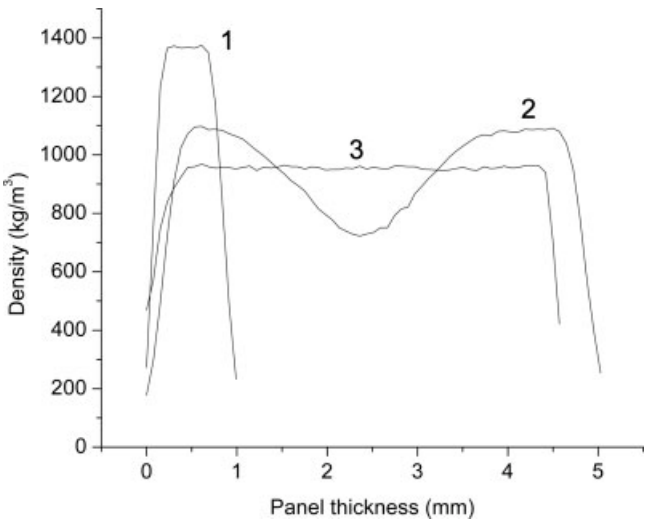

Figure 3 Comparison of the density profiles between compression-molded sugarcane fiber–HDPE composites and extruded commercial wood–HDPE composites. (1) 1-mm-thick composites with 30 wt % sugarcane fiber, (2) 4.5-mm-thick composites with 30 wt % sugarcane fiber, and (3) 17.5-mm-thick commercial composites with about 40 wt % wood fiber.

ally entangled together. Most of EBF had a broom-like structure around the rough surface due to the mechanical cutting during the fiber preparation [Fig. 1(c)]. Hence, RBF and PRF had a clear profile with respect to EBF. For all the sugarcane fibers, the number of fines (e.g., fiber segments and damaged fibers) significantly increased after the compounding process [Fig. 1(b, d)]. Also, entangled threads-like EBF (i.e., microfibril coils) were produced [Fig. 1(d)]. The maintained broom structure of EBF might enhance mechanical interlocking with the HDPE resins. The short fibers (larger than 60# in mesh size) had a granule shape with little change in dimension before and after compounding [Fig. 1(e, f)]. After compounding, EBF and RBF were light yellow in color, whereas PRF had a brown color.

Figure 2 presents the fiber dimension distributions of the RBF–HDPE blends before and after compounding. According to the cumulative distribution function (cdf), the sugarcane fiber distribution in the length and diameter before and after compounding fitted a lognormal distribution as follows,[29]

$$f(X|\mu,\sigma) = \frac{1}{X\sqrt{2\pi\sigma^2}}\exp\left[-\frac{(\ln X - \mu)^2}{2\sigma^2}\right] \quad (1)$$

TABLE III
Mechanical Properties of Sugarcane Fiber/HDPE Composites

HDPE resin	Fiber	Mesh size	Flexural storage modulus E' (GPa)	Tensile strength (MPa)	Izod impact strength (J/m)
HDPE resins					
HD9856B	–	–	1.86 (0.10)	32.30 (1.23)	73.84 (6.21)
HD6761	–	–	1.61 (0.07)	29.54 (0.94)	39.68 (1.51)
HD6714	–	–	1.43 (0.09)	25.14 (1.65)	36.04 (3.58)
HD6733	–	–	1.25 (0.06)	13.42 (1.49)	25.04 (4.57)
Sugarcane fiber/HDPE composites					
HD9856B	RBF	+20#	2.30 (0.15)	26.19 (1.66)	41.91 (5.64)
		−#06+/02	2.75 (0.12)	23.96 (1.57)	46.76 (2.86)
		−#06	2.62 (0.14)	23.58 (1.61)	30.19 (0.49)
	PRF	+20#	2.49 (0.09)	21.57 (1.28)	45.86 (8.18)
		−#06+/02	2.68 (0.28)	20.81 (1.50)	47.10 (2.60)
		−#06	2.63 (0.16)	18.23 (0.81)	31.39 (2.11)
	EBF	+20#	2.77 (0.16)	24.36 (3.24)	60.90 (8.27)
		−#06+/02	2.82 (0.26)	23.56 (0.86)	54.88 (7.11)
		−#06	3.02 (0.11)	20.98 (1.69)	48.65 (8.20)
HD6761	RBF	+20#	2.78 (0.07)	22.29 (1.43)	32.82 (3.60)
		−#06+/02	2.44 (0.08)	22.30 (1.29)	32.53 (3.28)
		−#06	2.42 (0.18)	21.07 (1.89)	20.51 (1.77)
	PRF	+20#	2.32 (0.18)	16.71 (1.63)	35.83 (3.69)
		−#06+/02	2.52 (0.11)	17.26 (1.42)	29.97 (4.14)
		−#06	2.29 (0.11)	15.15 (1.34)	21.19 (3.14)
	EBF	+20#	2.34 (0.21)	24.43 (4.11)	38.15 (5.97)
		−#06+/02	2.34 (0.23)	21.62 (1.78)	37.62 (5.87)
		−#06	2.65 (0.08)	26.29 (1.18)	33.40 (2.72)
HD6714	RBF	+20#	2.40 (0.12)	20.73 (1.41)	28.38 (4.37)
		−#06+/02	2.55 (0.11)	21.36 (1.58)	26.22 (2.43)
		−#06	2.34 (0.33)	18.13 (1.06)	19.51 (2.15)
	PRF	+20#	2.11 (0.09)	16.39 (1.70)	29.33 (1.79)
		−#06+/02	2.17 (0.37)	15.43 (1.29)	27.46 (2.98)
		−#06	2.12 (0.16)	15.50 (0.95)	18.75 (1.07)
	EBF	+20#	2.43 (0.13)	23.51 (3.33)	38.60 (1.88)
		−#06+/02	2.55 (0.14)	19.68 (1.58)	35.24 (6.16)
		−#06	2.51 (0.05)	19.66 (1.15)	28.42 (4.55)
HD6733	RBF	+20#	2.50 (0.14)	18.81 (2.42)	25.43 (3.79)
		−#06+/02	2.41 (0.12)	18.45 (1.13)	26.22 (2.43)
		−#06	2.35 (0.14)	17.30 (0.80)	19.51 (2.15)
	PRF	+20#	2.10 (0.16)	13.15 (1.98)	28.02 (3.48)
		−#06+/02	2.04 (0.19)	12.33 (1.42)	22.15 (2.51)
		−#06	1.98 (0.03)	11.44 (1.93)	17.91 (1.05)
	EBF	+20#	2.39 (0.21)	17.16 (2.77)	33.52 (8.90)
		−#06+/02	2.21 (0.18)	19.22 (1.05)	31.49 (5.33)
		−#06	2.29 (0.12)	17.86 (1.87)	26.17 (3.87)

RBF, raw bagasse fiber; PRF, pure rind fiber; and EBF, alkali-extracted bagasse fiber. The values in the parentheses are standard deviations.

where $f(X)$ is the probability density function (pdf) of X. The independent variable, X, is the fiber length or diameter with the unit of millimeter ($X \geq 0$). In eq. (1), μ and σ are the location and shape parameters, respectively.

For both length and diameter, the sample distributions after compounding had a left shift with respect to those before compounding (Fig. 2). For the length, the broad distribution range before compounding was narrowed to a small range after compounding [Fig. 2(a)], thus the concentration of the short fibers significantly increased. For the diameter, the distribution range after compounding also shifted to the left, but was close to that before compounding [Fig. 2(b)]. The shift in the fiber dimension distribution was probably ascribed to the shear stresses and friction force between the fibers and HDPE resins during compounding. Hence, the amount of short fibers with a small diameter significantly increased after compounding (Fig. 2).

As shown in Table II, the sugarcane fibers decreased in the dimension after compounding. The long fibers (i.e., +20#) had a large decrease in length and diameter, whereas the short fiber (i.e., −20/+60# and −60#) had less change in dimension [Table II]. Similarly, the long fibers also had a significant decrease in the aspect ratio after compounding. However, the short fibers had less change in the aspect ratio after compounding (Table II). For instance, the +20# mesh size RBF decreased from 3.01 mm to 0.91 mm in length on average and its aspect ratio decreased by 204% after compounding, while the −20/+60# mesh size RBF fibers only decreased by 29% in aspect ratio. However, there was little change for the −60# mesh size RBF after compounding (Table II).

Mechanical properties of the resultant composites

As shown in Figure 3, the density profile of compression-molded sugarcane fiber/HDPE composites was directly related to the thickness. With a large thickness, the density gradient of the compression-molded composites was built up along the center of thickness due to the temperature difference between the center and surface of composites during pressing. Sugarcane fiber/HDPE composites with the 4.5 mm thickness presented a shoulder shape on the density profile. Like the extruded commercial composites, however, the 1-mm-thick composites had an almost uniform density across the thickness except for the surface layers (Fig. 3).

For a binary system (only including the fiber and polymeric matrix), the tensile modulus of composites, E_c, of the resultant composites is related to the fiber and polymeric matrix properties as,[30]

$$E_c = E_f\left(1 - \frac{W_m\rho_c}{\rho_m}\right) + E_m\frac{W_m\rho_c}{\rho_m} \quad (2)$$

where E_f and E_m are the tensile moduli of the fiber and matrix, respectively. W_m is the weight fraction of the matrix, while ρ_c and ρ_m are the density of the composite and matrix, respectively. In this study, ρ_c, ρ_m, and E_f were known, and W_m was fixed to be 30 wt %. For the specific polymeric matrix, therefore, E_c was proportional to the value of E_m.

Since the flexural storage modulus (E') of the resultant composites has a proportional relationship with E_c, E' was proportional to E_m of the HDPE resins, whereas it was not sensitive to the fiber type and mesh size (Table III). Composites with HD9856B had the highest E' value on average. Composites with HD6761 were stronger in stiffness than those with HD6714 and HD6733. However, composites with HD6733 had the lowest E' value on average. As a result, the stiffness of the resultant composites increased with an increase in the E_m values at the same fiber content.

The tensile strength of the resultant composites was also related to the resin type (Table III). Composites with HD9856B had the highest tensile strength, while composites with HD6761 had better performance in tensile strength than those with HD6714 and HD6733.

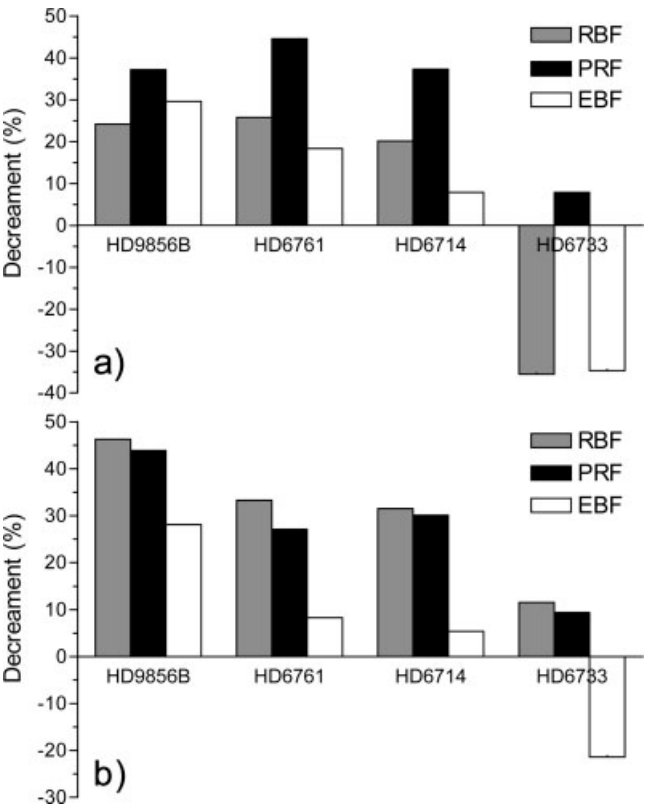

Figure 4 Comparison of the influences of fiber and resin types on (a) tensile strength and (b) impact strength of sugarcane fiber–HDPE composites.

Composites with HD6733 had the lowest tensile strength in the resultant composites. The combination of the resin type, fiber type, and fiber mesh size also influenced the mechanical properties of the resultant composites. With the same HDPE resin, composites made from the fiber with a large mesh size (i.e., −60#) had a lower tensile strength on average, while those with a small mesh size (i.e., +20#) had a higher tensile strength on average (Table III). Moreover, the tensile strength of PRF-reinforced composites was smaller than that of RBF- and EBF-reinforced composites with the same HDPE resin.

Composites with HD6761, HD6714, and HD6733 mostly failed with a complete fracture under the impact load; whereas composites with HD9856B usually had a hinged fracture, indicating stronger impact strength. Furthermore, the impact strength was sensitive to the fiber type and mesh size. Composites with the long fibers (e.g., +20#) had higher impact strength than those with the short fibers (e.g., −60#). With the same fiber mesh size and HDPE resin, EBF-reinforced composites had higher impact strength than RBF- and PRF-reinforced composites (Table III).

As shown in Figure 4, the strength properties of the resultant composites were related to the resin type, the fiber type, and the compatibility between the fibers and HDPE resins. Incorporation of the fibers in HD9856b, HD6761, and HD6714 significantly decreased the tensile and impact strengths (Fig. 4). For the HDPE resins, composites with PRF and RBF had a

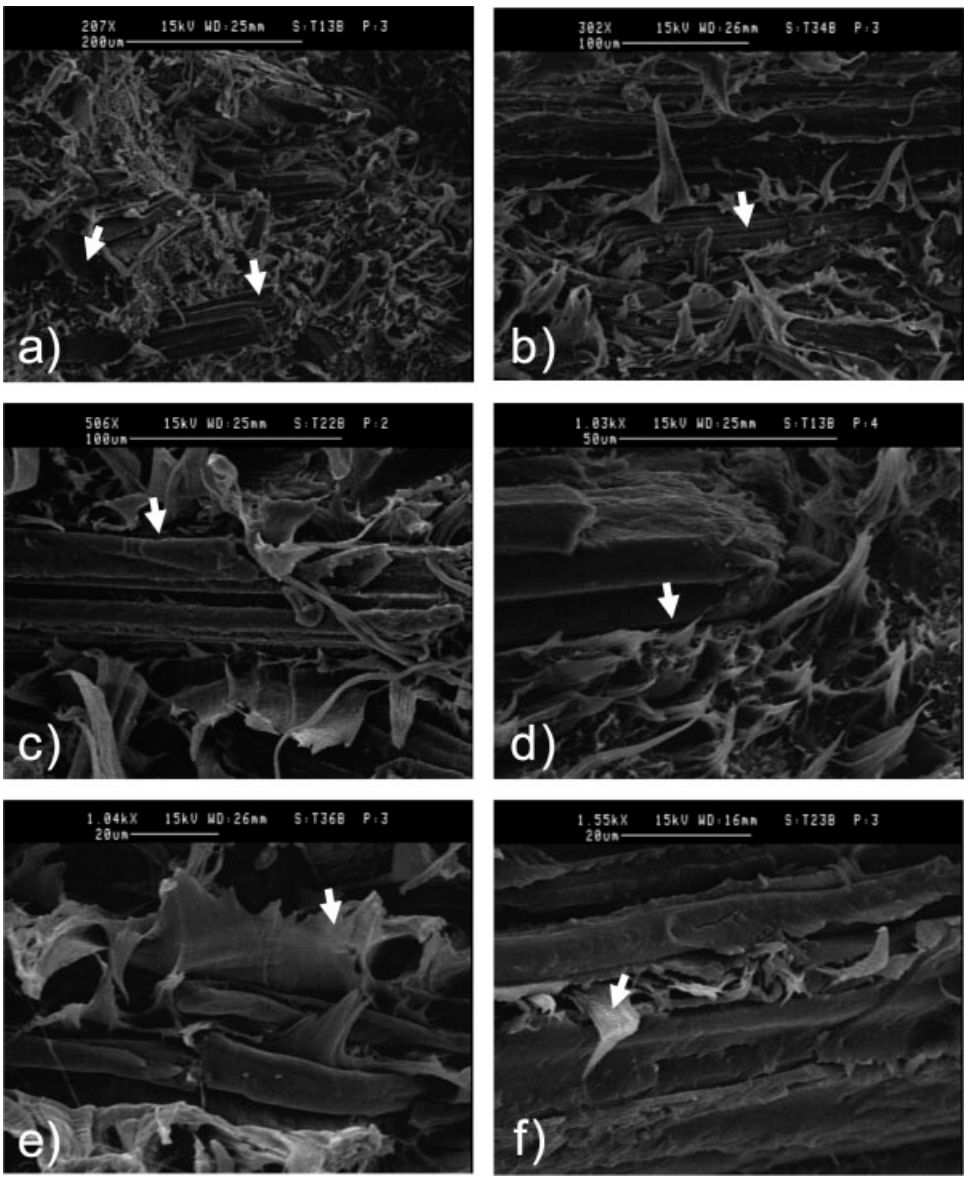

Figure 5 SEM micrographs for fracture surfaces of the sugarcane fiber–HDPE interface after tensile testing. (a) +20# PRF in HD6733 (207×), (b) +20# EBF in HD6761 (302×), (c) +20# PRF in HD6714 (506×), (d) +20# PRF in HD6733 (1030×), (e) −60# EBF in HD6761 (1040×), and (f) −20/+60# PRF in HD6714 (1550×).

large decrement in both strengths with respect to those with EBF. The maximum decrease in both strengths was over 40%.

In the HD6733 resin, however, EBF improved both tensile and impact strengths on average by 34.7% and 21.4%, respectively, whereas RBF improved the tensile strength on average by 35.5% but had a negative effect on the impact strength. PRF, however, had a detrimental effect on the strength properties of the resultant composites (Fig. 4). The increment in both strengths in the HD6733 resin may be due to the fact that thermoplastic polymers with a short molecular chain relatively decreased the *in situ* gaps at the interface and improved the interfacial compatibility as a dispersing agent,[31] and thus improving the mechanical performance at the interface.

SEM micrographs after the tensile and impact testing are shown in Figures 5 and 6, respectively. The SEM micrographs after the tensile testing presented the fracture surfaces similar to those after the impact testing. However, the tensile fracture surfaces were rougher than the impact fracture surfaces. The sugarcane fibers were either pulled out with smooth grooves left in the matrix [Fig. 5(a) and 6(a)] or imbedded in the matrix [Fig. 5(b) and 6(b)]. Some fibers were pulled out and broken [Fig. 5(a)]. After testing, most of the fibers had a clear profile in the HDPE resins. Also, there was a clear border between the fibers and HDPE resins [Figs. 5(c), 5(d), and 6(c)]. Under a high magnification number, the gaps between the fibers and HDPE resins were clearly shown in Figures 5(d) and 6(c). Some HDPE resins penetrated into the gaps between the fibers and even the cell lumens of the fibers [Fig. 5(e, f)], but they did not pass through the pit lumens [Fig. 6(d)]. All the SEM micrographs indicated that the fibers were enveloped or surrounded by the bulk of the HDPE resins, and they only had a mechanical connection with the HDPE resins. The fiber–HDPE interface may be strengthened with mechanical interlocking.[28,31]

According to the ANOVA analysis on the tensile strength, the main effects of MFI (or the resin type) and the fiber type and mesh size were significant at the 95% confidence interval. The interaction effect of the fiber type and mesh size was not significant, but the other interaction effects were significant (Table IV). Similarly, all the main effects of MFI and the fiber type and mesh size were significant for the impact strength. However, all the interaction effects were not significant (Table V).

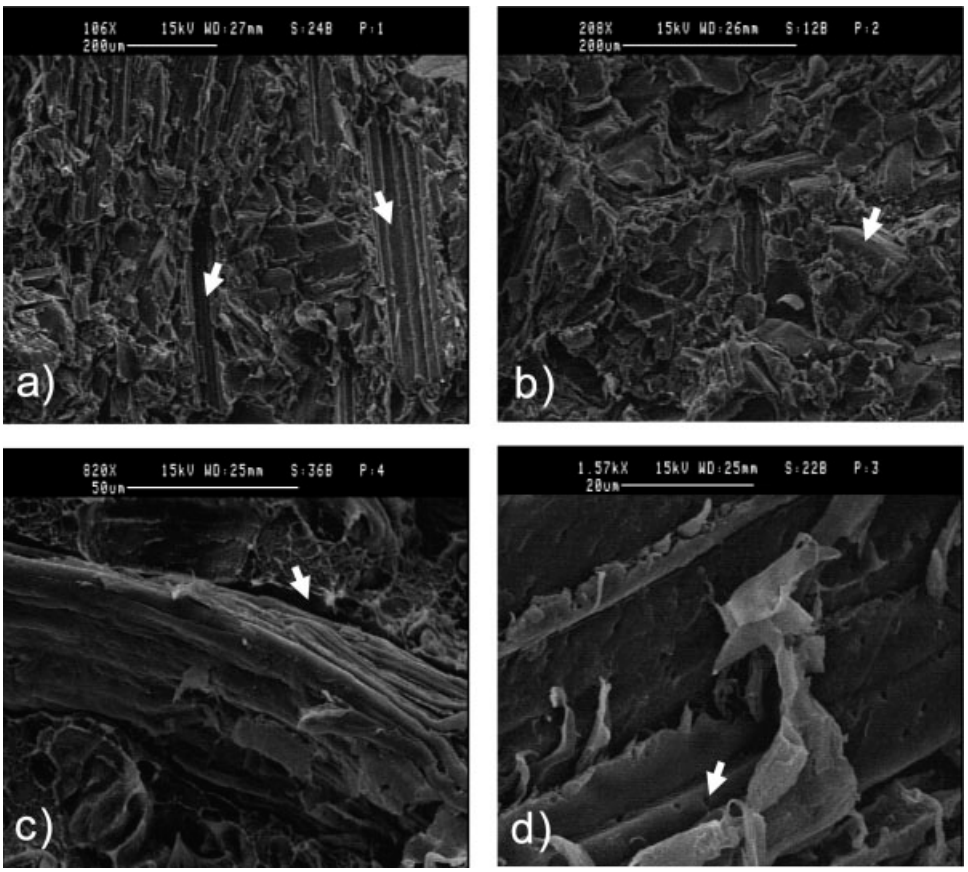

Figure 6 SEM micrographs for fracture surfaces of the sugarcane fiber–HDPE interface after impact testing. (a) −60# PRF in HD6714 (106×), (b) −60# RBF in HD6733 (208×), (c) −60# EBF in HD 6761 (820×), and (d) +20# PRF in HD6714 (1570×).

TABLE IV
Three-Way ANOVA on the Tensile Strength of the Resultant Composites

Source	DF	Type III sum of square	Mean square	*F* value	Pr > *F*
Model	35	2736.88	78.20	20.16	< 0.0001
MFI	3	1128.36	376.12	96.95	< 0.0001
Type	2	1238.59	619.30	159.63	< 0.0001
MFI*Type	6	148.20	24.70	6.37	< 0.0001
Size	2	89.34	44.67	11.51	< 0.0001
MFI*Size	6	50.37	8.39	2.16	0.0487
Type*Size	4	20.73	5.18	1.34	0.2584
MFI*Type*Size	12	132.23	11.02	2.84	0.0014
Error	175	678.93	3.88		

MFI, melt flow index; Type, fiber type; Size, fiber mesh size; DF, degrees of freedom; *F* value, the value of F test; Pr, *P* value, i.e., the power of F test.

Effect of the melt flow index

As aforementioned, MFI of the HDPE resins had a significant influence on the mechanical properties of the resultant composites according to the statistical analysis (Tables IV and V). MFI is an indirect measurement of the molecular weight and structure of thermoplastic polymers. In general, a HDPE resin with a small MFI value has a high molecular weight and long molecular chain.

The long molecular chain and high molecular weight help improve the interfacial adhesion between HDPE macromolecules by polymer chain entanglement. Furthermore, The HDPE resins with a long molecular chain and high molecular weight significantly enhance the absorption energy to the impact load with respect to the HDPE resins with a short molecular chain and low molecular weight, thus resulting in the improvement of the impact strength. It has been reported that the impact strength was proportional to the molecular weight of linear polyethylene polymers.[32] Accordingly, both the strength and stiffness of the HDPE resins normally increase with decreasing MFI.[33,34]

For most sugarcane fiber/HDPE composites, the tensile strength decreased with an increase in MFI [Fig. 7(a) and Table III]. The composites with HD9856B had the highest tensile strength on average, but the composites with HD6733 had the lowest tensile strength. Composites with HD6761 and HD6714 had higher tensile strength than composites with HD6733.

Similar to the tensile strength, the impact strength for most sugarcane fiber/HDPE composites decreased with an increase in MFI [Fig. 7(b) and Table III]. Composites with HD9856B had the highest impact strength on average, whereas composites with HD6733 had the lowest impact strength. Composites with HD6761 and HD6714 were between these two composites in the impact strength. According to the experimental results (Table III), the mechanical performance of the HDPE resins at the interface was ranked as follows: HD9856B > HD6761 > HD6714 > HD6733.

Effect of the sugar content

Figure 8 shows the HPLC characteristics of chemical analytes in the sugarcane fibers. The primary sugar composition in the sugarcane fibers was sucrose, glucose, and fructose. For standard 1, sucrose had a big and strong peak at the retention time of about 7.7 min,

TABLE V
Three-Way ANOVA on the Impact Strength of the Resultant Composites

Source	DF	Type III sum of square	Mean square	*F* value	Pr > *F*
Model	35	17520.84	500.60	24.03	< 0.0001
MFI	3	10062.40	3354.13	161.01	< 0.0001
Type	2	3463.92	1731.96	83.14	< 0.0001
MFI*Type	6	173.63	28.94	1.39	0.2230
Size	2	3474.58	1737.29	83.40	< 0.0001
MFI*Size	6	243.25	40.54	1.95	0.0774
Type*Size	4	195.98	48.99	2.35	0.0570
MFI*Type*Size	12	191.11	15.93	0.76	0.6858
Error	141	2937.21	20.83		

MFI, melt flow index; Type, fiber type; Size, fiber mesh size; DF, degrees of freedom; F value, the value of F test; Pr, *P* value, i.e., the power of F test.

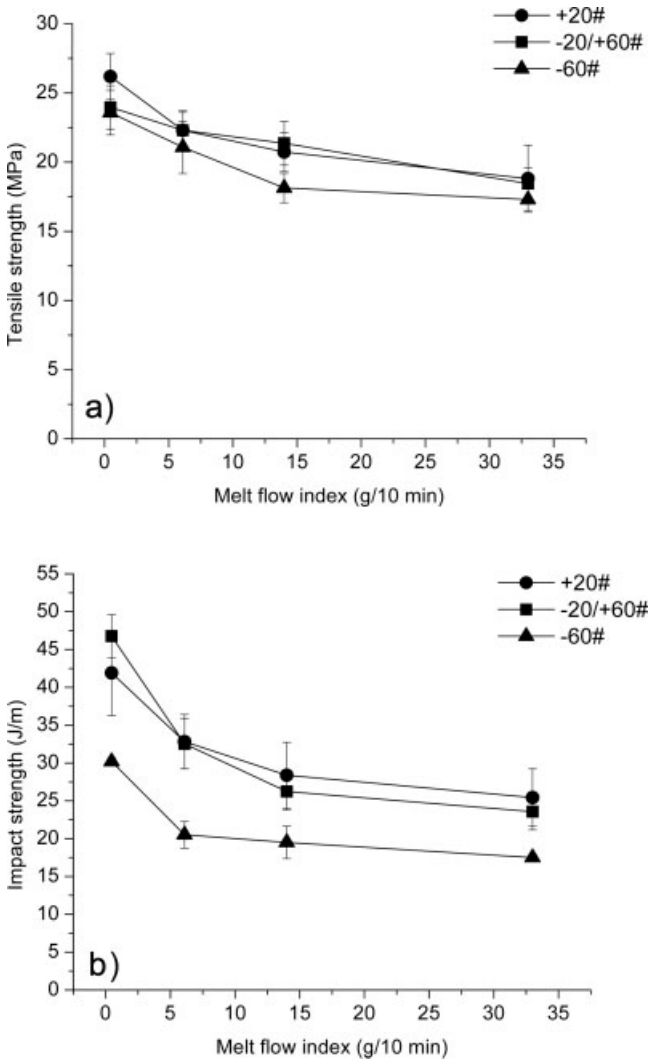

Figure 7 Effect of MFI on (a) tensile strength and (b) impact strength of RBF–HDPE composites.

while the moderate feature peaks of glucose and fructose occurred at 10.7 and 11.7 min, respectively. PRF clearly presented these peaks, and had more sucrose than glucose and fructose. However, RBF and EBF had very weak signals of these three compounds. Hence, PRF significantly differed from RBF and EBF in the sugar content. Hunsigi[35] estimated that the sucrose content of the pure rind fiber was over 10%, but that of the fresh bagasse fiber was between 2 and 3%. In this study, the sucrose content of PRF was as high as 16.4 wt %. It also contained 1.9 wt % glucose and 3.3 wt % fructose. The sugar components of RBF were mostly removed after the sugar extraction process and further degraded for a period of open-door storage. EBF did not contain these three compounds because of alkali extraction. Thus, the amount of these compounds in RBF and EBF can be neglected (Table VI).

The sucrose content in the fibers significantly influenced the tensile strength of the resultant composites. Compared with composites with RBF and EBF, composites with PRF had a dramatic decrease in the tensile strength for all the HDPE resins due to the high sucrose content in PRF [Fig. 4(a) and Table VI]. PRF decreased the tensile strength by 45% on maximum with respect to both RBF and EBF, which contain little sucrose. However, the impact strength was not sensitive to the sucrose content [Fig. 4(b) and Table VI].

Effect of the fiber type

The fiber type had a significant influence on the tensile and impact strengths according to the statistical analysis (Tables IV and V). PRF contained more sucrose, while RBF had some sucrose (Fig. 8 and Table VI) and many pith residuals. In addition, RBF had less hemicellulose with respect to PRF.[5,6] Most of pith, hemicellulose, and sucrose were removed from EBF, but both RBF and PRF contained more hemicellulose with respect to EBF, which might be harmful to the interfacial adhesion. Since RBF used was stored outdoors for long time, some elements (e.g., pith, sucrose, and hemicellulose) in the sugarcane fibers were decomposed or leached out under the outdoor weather conditions. Therefore, RBF contained few components detrimental to the interface with respect to PRF. Because of the chemical composition difference, RBF, PRF, and EBF had different performance in the resultant composites. In this study, EBF and RBF showed a better performance as filler in the HDPE resins than did PRF (Table III).

Effect of the fiber dimension and aspect ratio

The mechanical performance of the resultant composites was also related to the fiber length and shape.

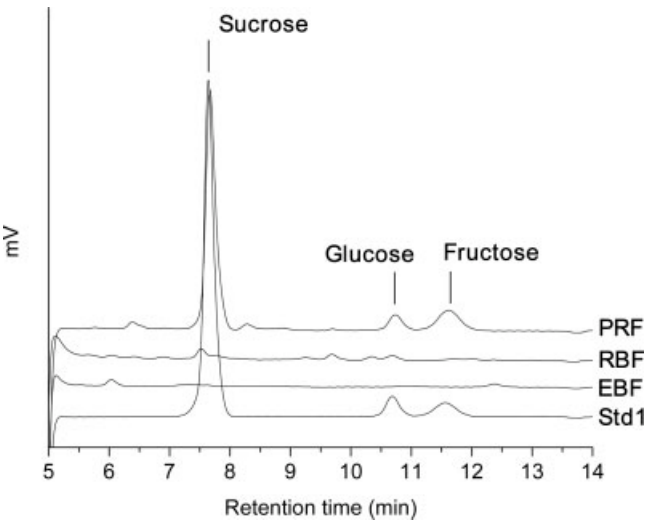

Figure 8 HPLC chromatographs of various sugarcane fibers. Std1, standard 1; RBF, raw bagasse fiber; PRF, pure rind fiber; and EBF, alkali-extracted bagasse fiber.

TABLE VI
Sugar Composition Analysis of Various Sugarcane Fibers

Fiber type	Dry materials (wt %)	Brix (wt %)	Sucrose (wt %)	Glucose (wt %)	Fructose (wt %)
RBF	92.80 (0.71)	2.53 (0.24)	0.09 (0.02)	0.10 (0.02)	0.05 (0.02)
PRF	94.30 (0.00)	29.83 (0.32)	16.38 (0.27)	1.94 (0.14)	3.25 (0.12)
EBF	93.15 (0.07)	1.03 (0.13)	0.03 (0.02)	0.01 (0.01)	0.00 (0.00)

RBF, raw bagasse fiber; PRF, pure rind fiber; EBF, alkali-extracted bagasse fiber.
The values in parentheses are standard deviations.

The long fibers had higher impact resistance and improved dimensional stability, whereas the short fibers had few flaws and therefore had higher strength per unit length.[30] The aspect ratio is an evaluation on the balance of the fiber length and shape. In general, the aspect ratio is proportional to the fiber length, but is inversely proportional to the cross section area. Zadorecki and Flodin[36] suggested that high fiber loading and fibers with an aspect ratio higher than the critical aspect ratio would be preferred for a sugarcane fiber/HDPE composite with high strength and stiffness. However, shear stresses during compounding may limit the distribution range of the fiber aspect ratio (Fig. 2 and Table II).

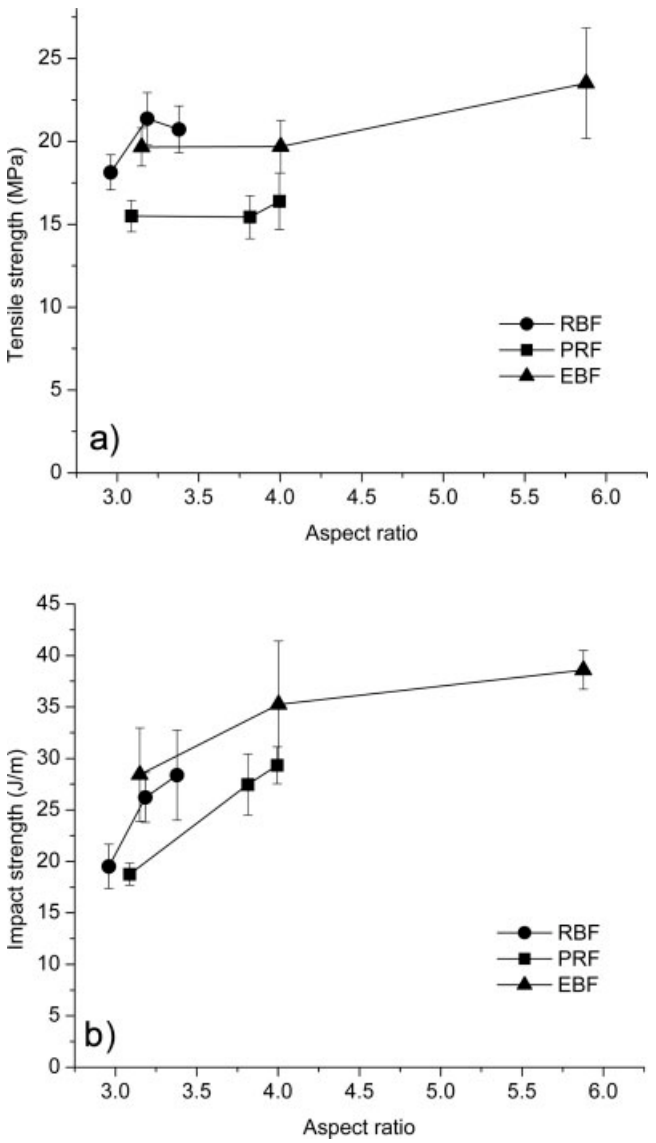

Figure 9 Relationships of the aspect ratio of the sugarcane fibers in the HDPE resin with (a) tensile strength and (b) impact strength of sugarcane fiber–HD6714 composites.

After compounding, the long fiber still had a large aspect ratio (Ca. 6.0), whereas the short fiber had an aspect ratio less than or close to three (Table II). The long fibers had a cylindrical tube form [Fig. 1(b, d)], whereas the short fibers were more like granules in shape [Fig. 1(f)]. The cylindrical tubes were more efficient to transfer the stresses at the interface with respect to the granule shape. Thus, the long fibers had a better reinforcement effect as filler in the HDPE resins compared with the short fibers.

As shown in Figure 9, both tensile and impact strengths were proportional to the aspect ratio. Composites containing EBF with a large aspect ratio had high tensile and impact strengths. At the same aspect ratio, EBF and RBF had a better performance in tensile strength in the HDPE resins with respect to PRF [Fig. 9(a)], while EBF had higher impact resistance than RBF and PRF [Fig. 9(b)]. In addition, EBF had a large aspect ratio range from 3.0 to 6.0, while PRF and RBF had a relatively narrow range from 3.0 to 4.0. This further indicated the morphological and dimensional effects of various sugarcane fibers on the strength properties of the resultant composites.

CONCLUSIONS

After the compounding process, the long fibers were a mixture of granules and cylindrical tubes in shape, whereas the short fibers were more like granules. A number of fines were produced after compounding. The length and diameter distributions of the sugarcane fibers followed the lognormal distributions. The long fibers significantly reduced the dimension and aspect ratio during compounding. Nevertheless, the short fibers had little change in the dimensional size

and aspect ratio after compounding. Although compounding influenced the fiber dimension and aspect ratio, it did not change the characteristics of the fiber dimension distribution.

The mechanical properties of sugarcane fiber/HDPE composites were mainly affected by the HDPE resin type and the fiber type, dimension, and aspect ratio. The tensile and impact strengths decreased with an increase in the MFI value. EBF and RBF had the better reinforcement in the HDPE resins than did PRF. PRF was detrimental to the interfacial bonding strength because of its high sucrose content. Hence, the long fibers with a large aspect ratio and low sucrose content would result in a better performance in the HDPE resins. However, the range of the fiber dimension and aspect ratio was limited by shear stresses during compounding. Moreover, all the fibers had variable performance in the HDPE resins because of the difference in the fiber dimension and aspect ratio after compounding. The poor mechanical performance of the sugarcane fibers indicated the inherent difficulty of good adhesion between the polar sugarcane fibers and nonpolar HDPE resins. Accordingly, chemical coupling treatment for the sugarcane fiber–HDPE interface would be necessary to improve the interfacial compatibility and adhesion.

We thank Mr. Ben Carrier in the Golden Chemical Company for supplying all the HDPE resins to support our research. Special appreciation is expressed to Dr. Donal Day and Mr. Brian White in the Audubon Sugar Institution, LSU Agricultural Center at St. Gabriel, LA for analyzing the sugar content of sugarcane fibers with HPLC.

References

1. Gilmore Sugar Manual; Sugar Publications: Fargo, ND, 2003.
2. van Dellewijn, C. Botany of Sugarcane; The Chronica Botanica Co.: Waltham, MA, 1952.
3. Barnes, A. C. The Sugar Cane; Wiley: New York, 1974.
4. Misra, D. K. In Pulp and Paper: Chemistry and Chemical Technology; Casey, J. P., Ed.; Wiley: New York, 1980; pp 504–631.
5. Anding, R. G. Masters Thesis, Louisiana State University, 1978.
6. Paturau, J. M. Bio-Products of the Sugar Cane Industry, 3rd ed.; Elsevier: Amsterdam, Netherlands, 1989.
7. Rowell, R. M. In Proceedings of the Fourth Pacific Rim Biobased Composites Symposium; Hadi, Y. S., Ed.; Bogor, Indonesia, November 2–5, 1998; pp 1–18.
8. Blackburn, F. Sugar Cane; Longman: London, UK, 1984.
9. Krzysik, A. M.; Youngquist, J. A. Int J Adhes Adhes 1991, 11, 235.
10. Youngquist, J. A.; Krzysik, A. M.; Muehl, J. H.; Carll, C. Forest Prod J 1992, 42, 42.
11. Rowell, R. M.; Keany, F. M. Wood Fiber Sci 1991, 23, 15.
12. Mclaughlin, E. C. J Mater Sci 1980, 15, 886.
13. Raj, R. G.; Kokta, B. V. Eur Polym J 1991, 27, 1121.
14. Nada, A.; Hassan, M. L. J Sci Ind Res 1999, 58, 616.
15. Hassan, M. L.; Rowell, R. M.; Fadl, N. A.; Yacoub, S. F.; Christainsen, A.W. J Appl Polym Sci 2000, 76, 575.
16. Stagel, G. C.; Tavares, M. I. B.; d'Alemeida, J. R. M. Polym Test 2001, 20, 869.
17. Paiva, J. M. F.; Frollini, E. J Appl Polym Sci 2002, 83, 880.
18. Collier, J. R.; Collier, B. J.; Thames, J. L.; Elsumi, M. M. Production and Evaluation of Sugarcane Fiber Geotxetiles, Report 1: Production and Laboratory Testing. Louisiana Transportation Research Center, Baton Rouge, LA, 1995.
19. Collier, J. R.; Collier, B. J.; Thames, J. L.; Elsumi, M. M. Production and Evaluation of Sugarcane Fiber Geotextiles, Report 2: Field Testing. Louisiana Transportation Research Center, Baton Rouge, LA, 1997.
20. Collier, J. R.; Collier, B. J. U.S. Pat. 5,718,802 (1998).
21. Chen, Y.; Chiparus, O.; Cui, X.; Calamari, T.; Screen, F. Presented at The 11th Annual International TANDEX Nonwovens Conference, The University of Tennessee, Knoxville, TN, November 6–8, 2001.
22. Chen, Y.; Chiparus, O.; Sun, L.; Negulescu, I. I.; Parikh, D. V.; Calamari, T. A. Int Sugar J 2004, 106, 86.
23. Han, G.; Wu, Q. Forest Prod J 2004, 54, 283.
24. Monteiro, S. N.; Rodriquez, R. J. S.; De Souza, M. V.; d'Almeida, J. R. M. Adv Perform Mater 1998, 5, 181.
25. Vazque, A.; Dominguez, V. A.; Kenny, J. M. J Thermo Comp Mater 1999, 12, 477.
26. International Commission of Uniformed Measurement of Sugar Analysis (ICUMSA) Standard GS7-23: Sucrose, Glucose, and Fructose in Sugarcane Molasses; Bartnes: Berlin, Germany, 2005.
27. Lu, J. Z.; Wu, Q.; Negulescu, I. I. J Appl Polym Sci 2004, 93, 2570.
28. Lu, J. Z.; Negulescu, I. I.; Wu, Q. Comp Interfaces 2005, 12, 125.
29. Casella, G.; Berger, R. L. Statistical Inference, 2nd ed.; Duxbury Press: Belmont, CA, 2001.
30. Kaw, A. K. Mechanics of Composite Materials; CRC Press: Boca Raton, FL, 1997.
31. Lu, J. Z.; Wu, Q.; McNabb, H. S. Wood Fiber Sci 2000, 32, 88.
32. McCrum, N. G.; Buckley, C. P.; Buchnail, C. B. Principles of Polymer Engineering; Oxford Science Publications: New York, 1997.
33. Wolcott, M. Forest Prod J 2003, 53, 25.
34. Viksne, A.; Rence, L.; Kalnins, M.; Bledzki, A. K. J Appl Polym Sci 2004, 93, 2385.
35. Hunsigi, G. Production of Sugarcane: Theory and Practice; Springer-Verlag: New York, 1993.
36. Zadorecki, P.; Flodin, P. Polym Eng Sci 1986, 7, 170.